Fault Interpretation Algorithm Using Frequency Response Analysis of Power Transformers

J. C. Gonzales, *Student Member, IEEE*, E. E. Mombello, *Senior Member, IEEE*

Abstract—Sweep Frequency Response Analysis (SFRA) is a powerful technique to detect mechanical damage in transformer windings, such as deformations and displacements, as well as other failures, helping to prevent severe damage. Since SFRA is a sensitive diagnostic technique, there are nowadays several commercially available measurement instruments to perform the tests, but the failure interpretation is usually based on expert opinion. One of the most advisable ways to face the task of interpretation of SFRA test results is the use of mathematical indexes to detect abnormalities along with an interpretation scheme. The failure interpretation methodology of SFRA tests must establish the possible relationships between frequency ranges and specific failures, because different failure types can be detected in different frequency ranges of the SFRA trace. This article proposes a new methodology for power transformer failure diagnosis using the relationships between the different decomposition levels of the original trace obtained by the use of the Discrete Wavelet Transform and the definition of frequency regions with variable limits, according the shape of the trace. Moreover, an interpretation map and a vector fitting analysis are also proposed in order to establish a specific failure.

Index Terms—Sweep Frequency Response Analysis, Power Transformers, Discrete Wavelet Transform, Frequency Regions, Vector Fitting, Expert Knowledge.

I. INTRODUCTION

Transformer diagnosis is a critical issue in maintenance scheduling in present power systems, which tend to a condition-based maintenance scheme. SFRA is a powerful and sensitive diagnosis technique for assessing the mechanical condition of windings and the iron core of power transformers, and it is increasingly being used in the power industry [1]. Unlike other techniques, the most important feature of SFRA lies in its ability to identify even minor faults, e.g. winding tilting, which makes it a promising tool for transformer diagnosis.

Most measurement devices used for transformer diagnosis include computer-aided failure detection tools, normally based on mathematical indexes, which are used according to standard procedures [2], [3], [4]. The measuring frequency normally ranges from 20 Hz to 2 MHz, which is the normally used transformer failure detection range [1]. The Relative Factor, the Correlation Coefficient (CC) and the Min-Max index (MM), are among the most used mathematical indexes for failure assessment. The abnormalities that may appear during SFRA trace comparison can be primarily observed as differences in transfer function traces. However, not all abnormalities should be linked to internal transformer failures because other factors may disturb the transformer's frequency response. Recent research works [5]-[6]-[7] which use mathematical indexes for failure detection show an increasing sensitivity by the use of these indexes, when evaluated on the proper frequency ranges. Thus, an important issue in the use of indexes is that disturbances and real failures should be differentiated.

This paper proposes a novel methodology for automatic failure detection and interpretation using SFRA. The automatic detection module based on the discrete wavelet transform for frequency response smoothing is presented in Section II. Section III presents a suitable definition of frequency regions limits, while Section IV proposes an interpretation map for electrical and mechanical failures. In Section V, a classification strategy for specific failures based on the Vector Fitting algorithm is presented. Section VI shows the validation of the proposed methodology by means of real case studies. Finally, conclusions are given in Section VII, where the methodology performance is evaluated. This work is complementary to the authors' recent publication [6].

II. FAILURE DETECTION MODULE USING DISCRETE WAVELET TRANSFORM DECOMPOSITION

The proposed scheme for power transformer diagnosis is depicted in Fig. 1.

In a recent research work [6], a new failure detection methodology using the DWT applied to SFRA has been introduced. For analysis purposes, a transfer function $H(\omega)$ has been defined. By applying the Discrete Wavelet Transform to the magnitude and phase of the transfer function (SFRA trace), smoothed transfer functions can be defined as in equations (1) and (2) [6].

$$\left|\bar{H}(\omega)\right|_{smooth} = \sum_{k \in Z} 2^{-M/2} \alpha_k \varphi_{\left|\bar{H}(\omega)\right|} (2^{-M}\omega - k) \qquad (1)$$

$$angle(\bar{H}(\omega))_{smooth} = \sum_{k \in Z} 2^{-M/2} \alpha_k \varphi_{angle(\bar{H}(\omega))} (2^{-M}\omega - k) \qquad (2)$$

For measurements using the "end to end" connection, the behavior of typical transfer functions at low frequencies is different from those of at medium and high frequencies, which suggests that the differences between transfer functions can also be different in various frequency regions.

J. C. Gonzales and E. E. Mombello are with the CONICET and the Instituto de Energía Eléctrica – Universidad Nacional de San Juan, Av. Lib.General San Martín 1109 Oeste, J5400ARL, San Juan – Argentina (e-mails: jgonzales@iee.unsj.edu.ar, mombello@iee.unsj.edu.ar).
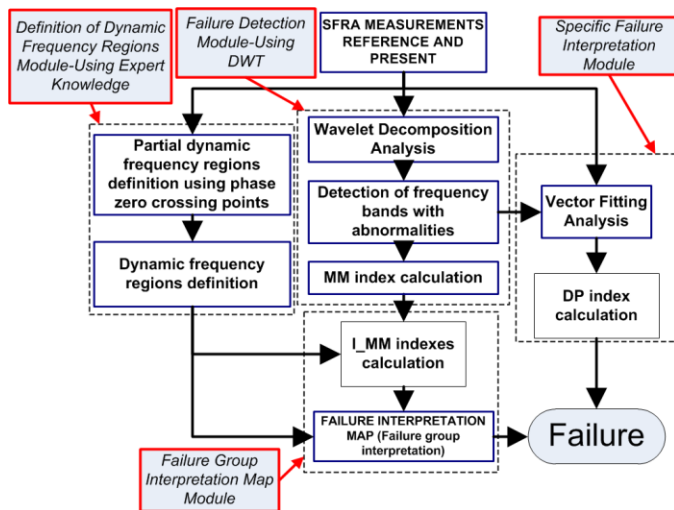
Fig. 1 Proposed diagnosis methodology scheme using SFRA.

In reference [6], DWT is applied to reference and present transfer functions using the 6th order Daubechies mother wavelet, and the corresponding smoothed versions of the transfer functions are obtained and compared. At each step of the smoothing process at a given decomposition level, DWT filters the trace without losing its most important information (i.e., it keeps the curve shape). The deviations between smoothed versions of the analyzed transfer function traces are evaluated at each decomposition level. These deviations are the true visual representations of the power transformer internal failures, because all other disturbances have been discarded, as discussed in [6]. The corresponding limits for failure differences $[\Delta i]_{limit}$ have been also defined in [6] as well as for CC and MM indexes, which were obtained by applying the decomposition procedure to real failure cases.

The detection algorithm is shown in Fig. 2. The detection procedure has seven decomposition levels, starting the analysis at the seventh level and ending at the first level (N=7:-1:1).
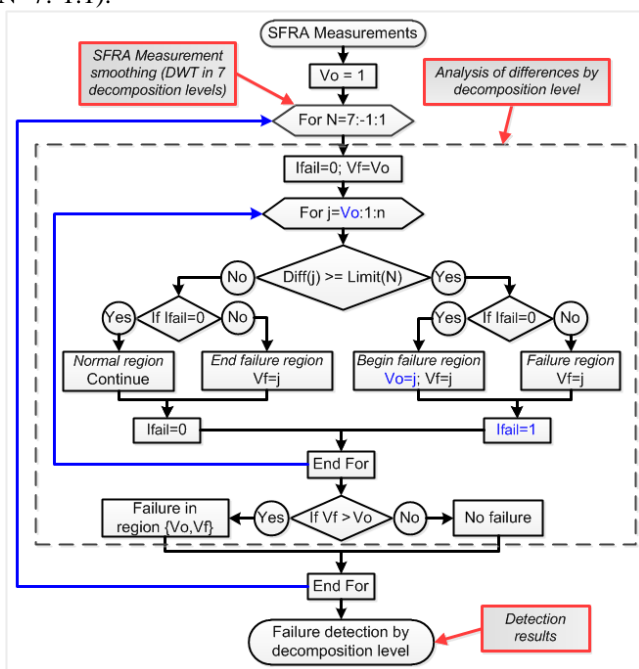

Fig. 2 Abnormality detection procedure at each decomposition level (DWT).

At each level, the smoothed transfer functions are compared. If any difference exceeding the limit ($[\Delta i]_{limit}$) is detected, the corresponding frequency band is saved. The frequency bands detected using this procedure at given decomposition levels are suitable for failure classification.

In addition, CC and MM indexes are calculated in this detection module. These indexes are calculated at each decomposition level, at the frequency band where the abnormality was detected. The resulting values are evaluated using the normal condition limits proposed in [6]. Any violation of these limits is a sign that the transformer is under some fault condition.

III. DEFINITION OF CLASSIFICATION FREQUENCY REGIONS USING EXPERT KNOWLEDGE

Research works [5] and [8] show how the variation of power transformer parameters influence on different frequency ranges of the transfer function. A change in parameter values are typically a consequence of failures [9]. Changes in the transformer frequency response may have different causes: a) Low frequency (LowF) trace shifts are normally due to changes in winding inductances and core structure; b) medium frequency (MedF) trace shifts indicate changes affecting the entire winding; and c) high frequency (HigF) trace shifts are due to changes in the series capacitances or in the measurement layout.

The classification frequency regions normally used for SFRA are fixed regions [2]. However, these frequency regions should not be considered as fixed, because they depend on the frequency response shape of the given transformer, which in turn depends on the power transformer structure and connection, as well as on winding type and voltage level. Thus, for a correct failure interpretation, a proper selection of classification frequency regions is required, which depends on the analyzed case.

A. Expert knowledge for proper selection of classification frequency regions

Typical transformer failures have been typified by CIGRE [1], IEC 60076-18-2012 [3] and IEEE standard C57.149-2012 [4]. Failures have been classified into electrical failures (denoted as EleF in Tab. 1) and mechanical failures (denoted as MecF in Tab. 2).

The following five frequency regions will be used in the analysis [8]-[9]: two low frequency regions, $LowF_1$ and $LowF_2$, a medium frequency region MedF and two high frequency regions, $HigF_1$ and $HigF_2$.

Failures mentioned in Tab. 1 and Tab. 2 are organized according the degree of influence of the given failure at the different frequency regions. Two scenarios can be established. In the first one, the failure affects only one frequency region (hereafter referred to as first classification level), e.g., an ungrounded core affecting only the $LowF_2$ frequency region. The second scenario includes failures affecting more than one frequency region (hereafter referred to as second classification level), e.g., a short circuit between turns affecting frequency regions $LowF_1$, $LowF_2$ and MedF. For electrical failures and

for the first classification level, three failure groups can be defined: failure group F_A for failures affecting only the $LowF_1$ region; group F_B for the $LowF_2$ region; and group F_C for the MedF region. For mechanical failures, other three failure groups are defined: group F_C for failures affecting only the MedF region; group F_D for the $HigF_1$ region; and F_E for the $HigF_2$ region. Other more complex failure groups could be proposed as well, considering, for example, the combination of the aforementioned groups. For instance, new groups could be: F_1 as a combination of F_A+F_B, F_2 as a combination of F_B+F_C, and so on.

Table 1. Electrical failure influence on frequency regions

EleF	$LowF_1$ F_A	$LowF_2$ F_B	MedF F_C	$HigF_1$ F_D	$HigF_2$ F_E
Short circuited (SC) turns	High	Low	Low	-	-
SC windings and core	High	Low	-	-	-
Ungrounded core	-	Low	-	-	-
Shorten core sheets	High	Low	-	-	-
Short circuit to ground		Low	Low	-	-

Table 2. Mechanical failure influence on frequency regions

MecF	$LowF_1$ F_A	$LowF_2$ F_B	MedF F_C	$HigF_1$ F_D	$HigF_2$ F_E
Winding Buckling	-	Low	High	Low	-
Tilt in conductors	-	-	Low	Low	-
Axial collapse	-	-	High	High	-
Loose clamping	-	-	-	High	-
Distorted leads	-	-	-	-	High

B. Limits of the classification frequency regions

The classification of failure groups requires identifying the five frequency regions ($LowF_1$, $LowF_2$, MedF, $HigF_1$ and $HigF_2$) for a given frequency response. This section provides a methodology to perform this task.

The frequency response behavior at low, medium and high frequencies is characterized by the presence of resonance peaks. The analysis of transfer functions shows a suitable correspondence between resonance peaks and phase zero crossing points, at low, medium and high frequencies.

Fig. 3 shows the frequency location of phase zero crossing points for a typical reference frequency response measurement. Phase zero crossing points represent an energy transfer between the inductances and capacitances of the windings. For low frequencies ranges, the point Pa represents the energy transfer between magnetizing inductances and shunt capacitances of the winding. For medium frequencies, at points Pb and Pc, the energy transfer occurs between winding inductances and shunt-series capacitances. In addition, the influence of winding coupling capacitances is predominant on this frequency range. For frequencies above Pc, which are considered as high frequencies, series capacitances are the most dominant influence.

Fig. 3 shows also the phase transitions from inductive to capacitive behaviors and vice versa. References [5] and [8] show relationships between failures and their influence on phase zero crossing points, because zero crossings cover different frequency ranges. Then, if the characteristic points

Pa, Pb, Pc and Pd are well defined, a preliminary failure interpretation becomes possible. It should be noted that the locus of a given characteristic point depends on the transfer function under analysis.

A methodology for the determination of the characteristic points has been proposed in [5]. References [5], [7] and [8] propose a possible sub-division of the main frequency regions (LowF and HigF) into sub-regions. The sub-divisions are as follow: the LowF region into sub-regions $LowF_1$ and $LowF_2$, defined in order to differentiate core influences and winding inductances and shunt capacitance influences. The HigF region is divided into regions $HigF_1$ and $HigF_2$, to differentiate series capacitances and measurement layout influences. The medium frequency range (MedF) of transformer transfer functions, especially in low voltage windings, covers a wide frequency range and it could contain several phase zero crossing points. Therefore, computing the mathematical index on this wide frequency range most probably will show no abnormalities (reduced abnormality detection sensitivity). This means that a significant number of failure detection and interpretation methods may have limitations [2]-[8]. Thus, MedF range can be divided into three sub-regions $MedF_1$, $MedF_2$ and $MedF_3$, depending on the characteristic points Pb and Pc. For failure interpretation, mathematical indexes are computed on these regions. However, only the result with highest sensitivity is used.

In order to know the frequency regions for a given trace, the frequency limits must be determined using the characteristic points.

Equation (3) is used for this task, expressed as a matrix for computation purposes.
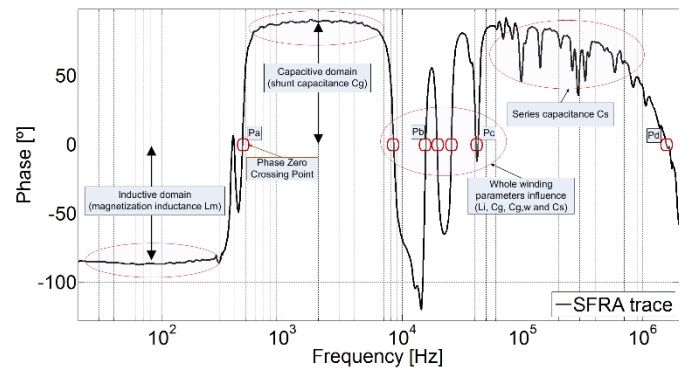

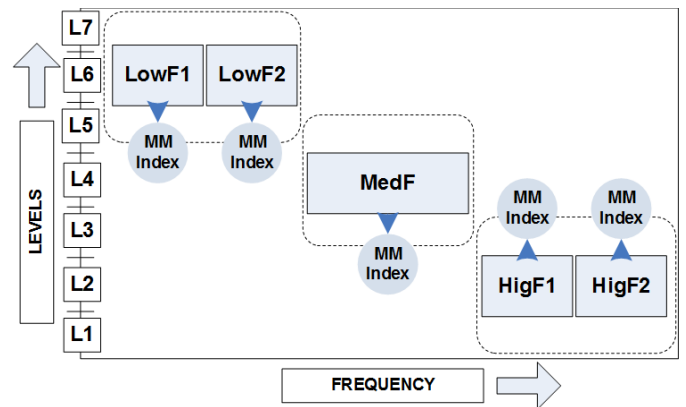Fig. 3. Selection of partial frequency regions using zero crossing points.

Fig. 4 Relation between decomposition levels and frequency ranges.

Here V is the matrix that contains the limits of the frequency regions obtained from the characteristic points Pa, Pb, Pc and Pd of the phase curve (SFRA trace).

In (3), the first, second and third rows of the matrix contain the low, medium and high frequency region limits, respectively. n is the number of frequency points measured, angle($H(\omega)$) is the angle of the measured transfer function and $fv(i)$ is the measurement point of the phase curve.

$$fv(i) = angle(\bar{H}(i))$$

$$i = 1.., Pa,.., Pb,.., Pc,.., Pd,..n - data$$

$$V_{\angle H(\omega)}(Pa,Pb,Pc,Pd) = \begin{bmatrix} \dfrac{fv(1)+Pa}{2} & \dfrac{Pa+Pb}{2} & 0 \\ Pb & \dfrac{Pb+Pc}{2} & Pc \\ Pd & fv(n) & 0 \end{bmatrix} \quad (3)$$

C. Failure detection procedure (DWT) based on classification frequency regions

Reference [6] shows the following relations between frequency regions and decomposition levels: low frequency regions $LowF_1$ and $LowF_2$ are related to decomposition levels L7 - L6 - L5; medium frequency regions $MedF_1$, $MedF_2$ and $MedF_3$ to decomposition levels L5 - L4 - L3; finally, high frequency regions $HigF_1$ and $HigF_2$ are related to levels L3 - L2 - L1. Thus, it is possible to relate the procedure for failure detection with the failure group interpretation stage, a necessary step for an automatic diagnostic algorithm.

The correlation between decomposition levels and frequency regions is shown in Fig. 4, firstly proposed in [6] and now applied in this work.

In this stage, the MM index is calculated for the classification frequency regions identified in the reference frequency response, which present no abnormalities.

Once the classification frequency regions and their corresponding MM index values have been determined, the identification of a given failure group is possible. In order to perform this sorting task, a failure interpretation map (FIM) is proposed in the next section.

IV. INTERPRETATION MAP FOR MECHANICAL AND ELECTRICAL FAILURES

Failures typified by experts (Tabs. 1 and 2) were presented in Section III.A, and the corresponding classification frequency regions have been identified in Section III.B. An interpretation map can be made based on the correlation between typified failures and classification frequency regions.

As explained above, transformer failures are classified into two general groups, namely, electrical failures and mechanical failures. Then, an interpretation map can be established for each failure mode. Some failure groups can be differentiated within each failure mode depending on their influence on the classification frequency regions. As detailed in Section III.A, failures affecting only one frequency region can be defined as belonging to the first level and failures affecting more than one region to the second level. Therefore, two classification levels are set in the interpretation map. In the first level,

failure groups are F_A, F_B and F_C are electrical failures while failure groups F_C, F_D and F_E are mechanical failures. The second classification level corresponds to failures affecting more than one classification frequency region. The electrical failure groups F_1 and F_2 are among this type of failures, affecting both low frequency regions and partially the medium frequency regions (LowF and MedF). Additionally, the mechanical failure groups F_3 and F_4 affect most of the higher part of the medium frequency regions and all high frequency regions (MedF and HigF). Other failure groups can be included on this interpretation map, as long as they can be typified.

Figure 5a and 5b show the interpretation maps for electrical failures, and Figure 5c and 5d the ones for mechanical failures, for SFRA measurements on the same phase of the transformer. Similar failure maps can be designed for measurements on different phases, using the failure limits determined in [6].

The main properties of failure interpretation can be summarized as follows (see Fig. 5): Each axis of the map represents a classification frequency region, defined and calculated in Section III. The value on each axis is computed using the I_MM index, calculated for the respective frequency range. Once the limits for normal condition have been established, an area on the map indicating the normal condition of the transformer can be defined.

The proposed I_MM index is computed by equation (4). The I_MM index ranges from 0 to 1, with 0 representing no difference and 1 the maximum difference between SFRA traces.

$$I\_MM(y_1, y_2) = 1 - MM(y_1, y_2)$$

$$= 1 - \dfrac{\sum\limits_{i=1}^{N} Min(|y_{1i}|,|y_{2i}|)}{\sum\limits_{i=1}^{N} Max(|y_{1i}|,|y_{2i}|)} \quad (4)$$

where y_{1i} and y_{2i} are the smoothed transfer function versions of the traces, as described in [6].

The I_MM index limits for transformer normal condition are: I_MM=1-0.91=0.09 for measurements on the same phases of the transformer, and I_MM=1-0.88=0.12 for measurements on different phases, because the failure limits of the MM index defined in [6] are 0.91 and 0.88 for measurements on the same and different phases, respectively.

Using the interpretation map, the failure group identification process has the following steps: After the classification frequency regions and the MM indexes have been calculated, the I_MM index is computed using (4) for each selected frequency region. A calculation of the I_MM indexes is first performed on the frequency bands showing abnormalities, using the previously calculated values of the MM index. Then, a second computation is made on the classification frequency regions showing no abnormalities. Once the I_MM indexes have been found and mapped in the interpretation map, the failure group can be determined. For the mapping process, straight lines are plotted for each calculated value of I_MM indexes. The intersection of the

lines indicate the failure group.

After having identified a failure group, the procedure continues in order to find a specific failure classification. With this aim, a classification analysis based on Vector Fitting is to be applied as explained in the next section.

V. SPECIFIC FAILURE INTERPRETATION USING VECTOR FITTING ALGORITHM

The interpretation map of Fig. 5 is designed to identify a failure group.

An analysis of resonance peak shifts within the detected frequency band with abnormalities is required to determine the specific failure within a given group. The Vector Fitting (VF) algorithm has been chosen for this task.

VF can found a complex rational function that best fits a transfer function defined by a discrete number of measurements, so that it allows to obtain a function that accurately represents the given frequency response [12]. The rational function obtained provides valuable information about the values and changes of power transformer parameters, as explained in [13]-[14]. The VF algorithm solves a nonlinear problem sequentially, representing it as a linear problem using the following approximation rational function,

$$\bar{H}_{SFRA}(j\omega) = h \cdot \left(\prod_{n=1}^{N+1} (j\omega - z_n) \right) \cdot \left(\prod_{n=1}^{N} (j\omega - p_n) \right)^{-1} \quad (5)$$

where z_n and p_n are the zeros and poles of $H_{SFRA}(j\omega)$, and h is a constant (real value).

In the iterative solution process, a Least Square Error (LSE) is obtained over a given frequency range. A suitable definition and an application of LSE is presented in [12], [13] and [14].

The poles, zeros and the residues of $H_{SFRA}(j\omega)$ can be calculated by means of equation (5). The application of VF to the analysis of shifts of resonance peaks of transfer functions can be found in [13]-[14].

In the proposed methodology, the goal of using VF is to determine a transfer function fitting with a minimum order of approximation that produces a minimum gap between poles loci and phase-zero crossing points, considering a specified LSE (optimal reproducibility). This condition ensures a satisfactory representation of the resonance peaks shifts, showing the typical behavior of winding inductances and capacitances. The identification of phase zero crossing points shifts also indicates changes of the winding parameters. Research works [13] and [14] analyze LSE as a function of the approximation order and the number of iterations. The application of VF to this problem can be summarized in seven steps as follows [13]:

1. Detect the frequency band with abnormalities (resulting from the failure detection module; see section II).
2. Identify the phase zero crossing points of the complex transfer function under analysis (resulting from the classification frequency bands definition; see section III).
3. Initialize the vector fitting order approximation N (N=4), NI number of iterations and LSE.
4. Apply the VF algorithm with an N-order approximation and NI iterations in the detected frequency band having

an abnormality (failure).
5. Calculate the shifting distances between pole locations and phase zero crossing points.
6. If the computed shifting distances have an error smaller than the pre-established LSE, then go to step 7; otherwise set N=N+2 and go back to step 4.
7. Save the pole location and show the plot.

The properties of the proposed method can be shown by means of a suitable example. Figure 6 shows a pole representation of SFRA traces of a 100 MVA_550/230 kV power transformer, plotted for the frequency range 100 Hz-10 kHz, where SFRA trace shifts have been detected.

The calculation procedure described above is firstly applied to the reference SFRA trace and, after a proper identification of pole locations, a VF approximation of the same order is used for the present SFRA trace. The optimal pole locations for this example is shown in Fig. 6, where the final result is N=20, LSE=0.000244 and NI=20.

The methodology proposed ensures a good representation of the shifts of resonance peaks, whether or not new poles appear, by locating the poles on the complex plane. Fig. 6 also shows a comparison between pole locations of SFRA reference and present traces, where poles are shifted towards low frequencies. A shift toward low frequencies is a natural capacitive behavior, since the capacitive values have increased, as noticed in [13], which most probably is to be linked to a short-circuit-to-ground failure. This specific failure interpretation is consistent with the results from the visual inspection of the transformer. As a corollary, this methodology turns to be very useful when transfer function shifts are not evident to expert's eye, as depicted in the example above (Fig. 6).

As the methodology proposed here is an automatic algorithm, vector fitting results are represented by a DP index, calculated using equation (6).

$$DP = \sum_{i=1}^{N} (R\_Poles(i) - P\_Poles(i)) \quad (6)$$

where R_Poles and P_Poles are the reference and present location of the poles. DP index calculation is an important part of the proposed interpretation methodology. Experts' experience can be summarized in Tabs. 1 and 2 for electrical and mechanical failures ([7], [13]). According to this, DP index can be characterized by a set of definitions, which have been firstly outlined in [8], [13] and [14] and now established in this work by means of the following rules.

A. At low frequencies regions (LowF_1 and LowF_2):

Rule-1.- Pole shifts toward higher frequencies represent an inductive behavior (decreasing values), so that the DP index is negative. Such shifts may be due to core problems or a short circuit (SC) between winding turns.

Rule-2.- Pole shifts toward lower frequencies represent a capacitive behavior (increased values), so that the DP index is positive. This behavior may be due to SC to ground or winding buckling.

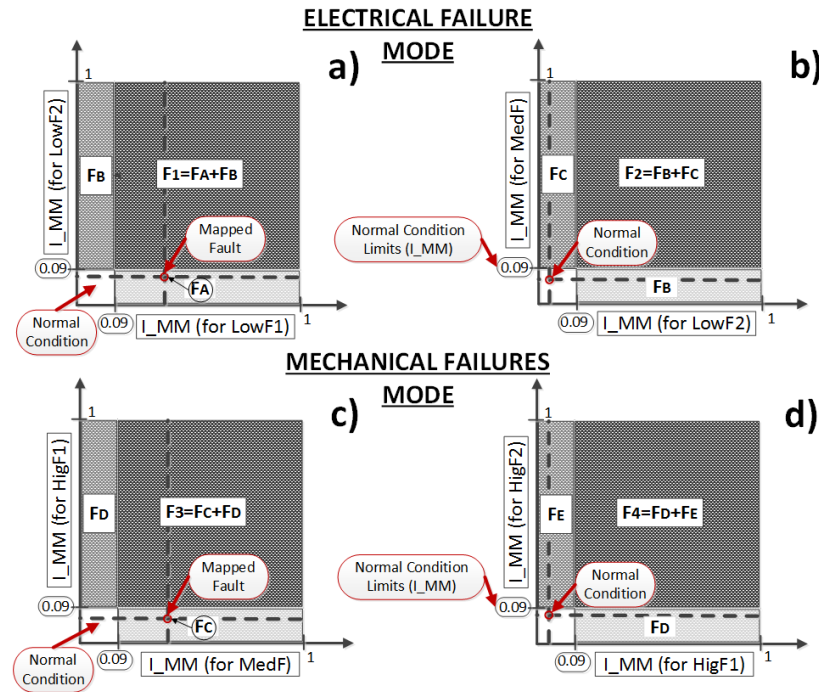### B. At mid-frequencies (MedF_1, MedF_2 and MedF_3):

Fig. 5 Interpretation map for electrical and mechanical failures.

Rule-1.-A positive DP value represents shunt-series capacitive increased values. Such shifts may be due to winding buckling, tilt of conductors or axial collapse.

Rule-2.-A negative DP value results from series-shunt capacitive decreased values or winding inductances decreased values. Failures producing such changes are SC between winding turns or winding compression.

C. At high frequencies (HigF₁):

C. At high frequencies (HigF$_1$):

Rule-1.-A positive DP value is mostly due to series capacitance increased values. Failures such as conductor tilting or axial collapse give rise to these changes in series capacitances.

VI. METHODOLOGY VALIDATION

The proposed methodology has been implemented using twenty-one measurements made on different transformers, as listed in Tab. 3, performed on the same phase and on different phases. The results of the application of the methodology are summarized in Table 3.

Table 3. SFRA measurements cases used to implement the methodology

Transformer	Frequency Range Hz	I_MM Index- Fault group	Condition result
100/100/33 MVA_550/230/14 kV	20-2x10e6	I_MM=0.06/0.75/0.19-F$_B$+F$_C$	Short circuit to ground fault
100 MVA_230 kV	20-2x10e6	I_MM=0.29/0.17/0.08- F$_C$+F$_D$	Tilting of winding wirings
30 MVA_145/13 kV	20-2x10e6	I_MM=0.55/0.75/0.08- F$_C$+F$_D$	Winding Buckling
750 MVA_420/27 kV	20-2x10e6	I_MM=0.43/0.85/0.17- F$_1$+F$_2$	Short circuit turns
25 MVA_115/24.9 kV	20-2x10e6	I_MM=0.07- Normal Condition	Normal condition
37 MVA_69/11 kV	20-2x10e6	I_MM=0.08- Normal Condition	Normal condition

150/150/60 MVA_240/60/13 kV	1x10e3- 1x10e6	I_MM=0.4/0.55/0.27- F$_1$+F$_2$	Short circuit turns
150/150/60 MVA_240/69/13 kV	1x10e3- 1x10e6	I_MM=0.03- Normal Condition	Normal condition
30 MVA_132/66/11 kV	20-2x10e6	I_MM=0.52/0.62/0.17- F$_C$+F$_D$	Tertiary winding movement
41.61 MVA_69/13.8 kV	20-2x10e6	I_MM=0.6/0.8/0.5- F$_1$+F$_2$	Short circuit turns
60/60/50 MVA_132/69/13.8 kV	1x10e3- 1x10e6	I_MM=0.065- Normal Condition	Normal condition
30 MVA_132/34.5/13.8 kV	1x10e3- 1x10e6	I_MM=0.041- Normal Condition	Normal condition
30 MVA_132/69/13.8 kV	1x10e3- 1x10e6	I_MM=0.09- Normal Condition	Normal condition
40 MVA_132/13.8 kV	100x10e3- 1x10e6	I_MM=0.34/0.78/0.20- F$_C$+F$_D$	Winding displacement
20/20/6 MVA_66/13.8/6.6 kV	1x10e3- 1x10e6	I_MM=0.02/0.58/0.67- F$_D$+F$_E$	Not typified Failure
10/15 MVA_33/13.8 kV	1x10e3- 1x10e6	I_MM=0.1-Normal Condition	Measurement problems
150/150/60 MVA_230/69/13.8 kV	1x10e3- 1x10e6	I_MM=0.61/0.5/0.38- F$_1$+F$_2$	Short circuit turns
30/30/10 MVA_132/34.5/13.8 kV	1x10e3- 1x10e6	I_MM=0.87/0.6/0.1- F$_C$+F$_D$	Wind. deformation-axial collapse
17 MVA_72/7.2 kV	1x10e3- 1x10e6	I_MM=0.22/0.79/0.03- F$_A$+F$_B$	Electrical failure-Not typified case
41 MVA_69/13.8 kV	1x10e3- 1x10e6	I_MM=0.51/0.45/0.18- F$_1$+F$_2$	Short circuit turns
30 MVA_138/13.8 kV	20-2x10e6	I_MM=0.88/0.31/0.03- F$_A$+F$_B$	Core problem-W. Normal Condition

Additionally, four different case studies have been taken into account for the validation. Two of them are presented in this section.

In the first case, the visual inspection of the power transformer revealed a short circuit between turns in the phase-S winding. In the second case, the visual inspection showed a winding conductor tilting.
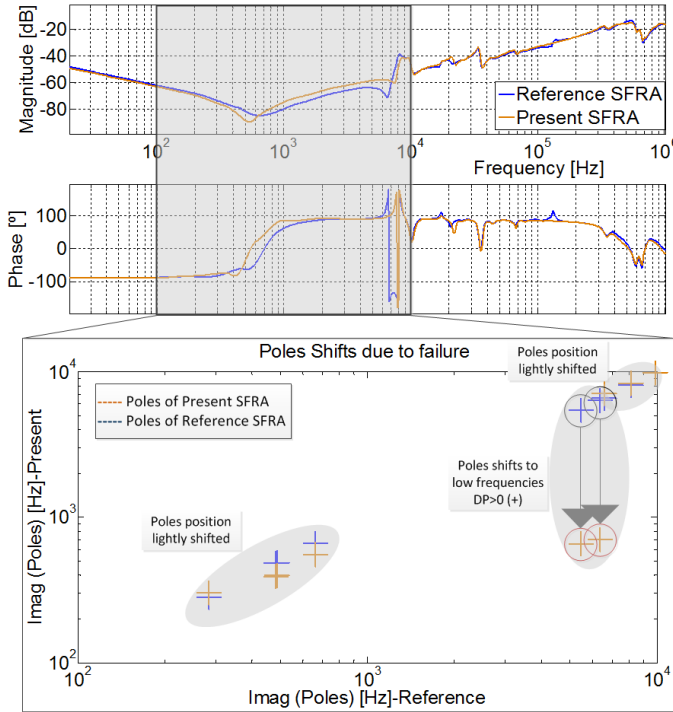
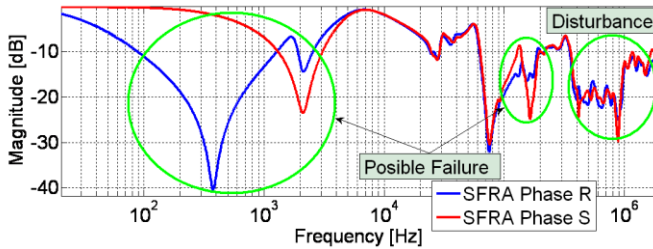Fig. 6 Pole shifts representation for short circuit to ground failure.

Fig. 7 SFRA measurement traces of a 750 MVA_420/27 kV transformer.
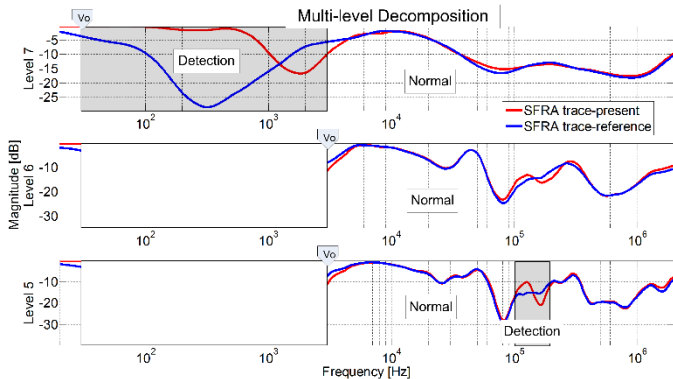

Fig. 8 Electrical failure mode detection using Multi-level Decomposition.

Case A: Fig. 7 shows the measurements on different phases at the low voltage side of a 750 MVA_420/27 kV power transformer. Phase R was considered the reference measurement for the analysis.

The results of applying the failure detection module are presented in Fig. 8, where only the last decomposition levels are shown. Abnormalities were found on the frequency region between 30 Hz and 3.08 kHz, corresponding to the 7th decomposition level. No new abnormality was found on the 6th decomposition level. An abnormality was found for the 114 kHz-178 kHz frequency range in the 5th decomposition

level. No abnormality was found for lower decomposition levels.

The following classification frequency regions have been identified for this case: LowF$_1$ (20 Hz-90 Hz), LowF$_2$ (90 Hz-5 kHz), MedF (5 kHz-900 kHz), HigF$_1$ (900 kHz-1 MHz).

The following I_MM index values have been calculated in the interpretation map module: I_MM=0.43 for the low frequency region LowF$_1$, I_MM=0.85 for the low frequency region LowF$_2$ and I_MM=0.17 for the mid-frequency region MedF. The failure has been identified on the interpretation map (a and b) as groups F$_1$+F$_2$, as shown in Fig. 9.

The final specific failure classification was performed using Vector Fitting (specific failure classification module). A short circuit between turns was detected as specific failure, because the index DP=-6.1487e+005 is smaller than zero, thus indicating an inductive behavior evidenced by pole shifts toward high frequencies, which agrees with the visual inspection of the transformer.

Case B: In the second case, measurements on the same phase (phase R) of the LV winding of a 100 MVA_550/230/14 kV transformer (see Fig.10).

The results of the application of the detection module is shown in Fig. 11, where an abnormality was detected at the 4th decomposition level in the 18 kHz-388.6 kHz range. No failure was found at lower decomposition levels. Minor differences above 1 MHz were not classified as failures.
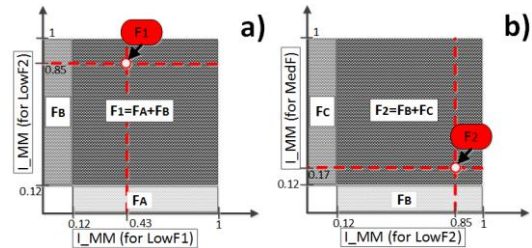

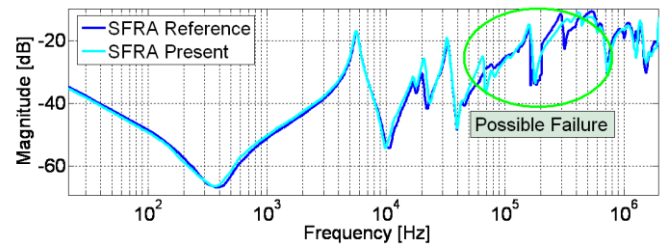Fig. 9 Failure group interpretation for Short Circuit between turns.

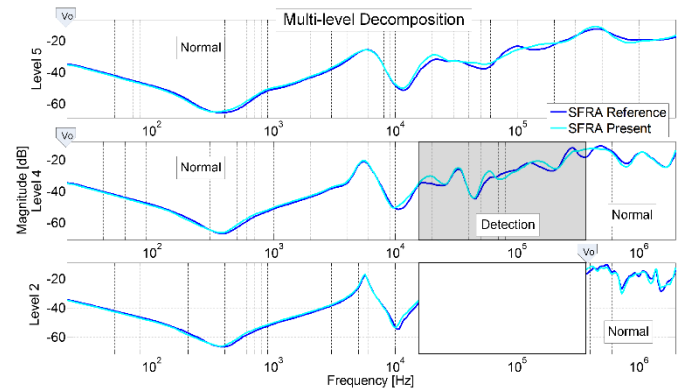Fig. 10 SFRA traces on a 100 MVA_550/230/14 kV power transformer.

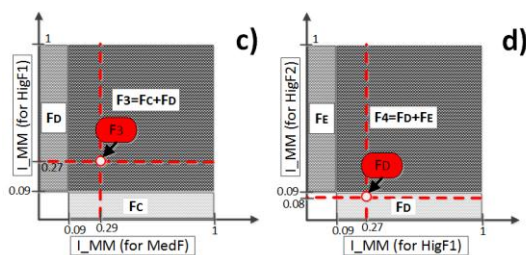Fig 11 Mechanical failure detection using Multi-level Decomposition.

Fig. 12 Specific failure group interpretation for conductor tilting.

The following classification frequency regions were identified by the corresponding module: $LowF_1$ (20 Hz-92 Hz), $LowF_2$ (92 Hz-2 kHz), MedF (2 kHz-40 kHz), $HigF_1$ (40 kHz-500 kHz) and $HigF_2$ (500 kHz-2 MHz). The calculated values for the I_MM index on the interpretation map module are: I_MM=0.29 for the mid-frequency region MedF, I_MM=0.27 for the region $HigF_1$ and I_MM=0.08 for the region HigF2. By applying the interpretation map (c and d), the failure was interpreted as belonging to the group $F_3= F_C+F_D$, as shown in Fig. 12.

The final specific failure classification has been achieved using the VF algorithm module, where the calculated value DP=4.5597e+004 is positive for medium and high frequencies, which represents series capacitance increased values. The methodology detects conductor tilting as specific failure, in agreement with the visual inspection of the transformer.

VII. CONCLUSIONS

An automatic methodology for failure detection and interpretation has been proposed in this work.

This methodology is based on a strategic application of the Discrete Wavelet Transform for transformer failure recognition. The application of the Discrete Wavelet Transform to the complex transfer function makes it possible a strategic sorting of SFRA trace abnormalities into different frequency ranges and different DWT decomposition levels. A methodology for the identification of suitable classification frequency regions for failure interpretation have been proposed. These regions are strategically correlated to each type of failure detected by the multilevel decomposition method.

An interpretation structure for failure group recognition has been proposed, using an interpretation map scheme composed of two classification levels, making it possible to recognize failure groups with different influence regions of the transfer function. The Vector Fitting algorithm has been applied to make a specific failure classification within a failure group, based on pole shifts analysis.

The proposed failure classification strategy is a complement to the power transformer diagnosis methodology based on SFRA presented in [6]. These tools make possible a more accurate detection and interpretation of SFRA results.

VIII. REFERENCES

[1] Working Group A2.26, "Mechanical-Condition Assessment of Transformer Winding Using Frequency Response Analysis (FRA)", CIGRE publication 2008.

[2] "Frequency response Analysis on Winding Deformation of Power Transformers", The Electrical Power Industry of People's Republic of China, Std. DL/T911-2004, ICS27.100, F24, Documents No.15182-2005, June 1st, 2005.

[3] International Standard, "Measurement of frequency response", IEC 60076-18, Switzerland 2012.

[4] IEEE Standards Association, "IEEE Guide for the Application and Interpretation of Frequency Response Analysis for Oil-Immersed", IEEE Power and Energy Society 2012.

[5] J. C. Gonzales and E. E. Mombello, "Automatic Detection of Frequency Ranges of Power Transformer Transfer Functions for Evaluation by Mathematical Indicators", IEEE PES T&D, Uruguay, September 2012.

[6] J. C. Gonzales and E. E. Mombello, "Detection of Failures within Transformers by FRA using Multi-resolution Decomposition", IEEE PES Transactions on Power Delivery, December 2013.

[7] J. Velasquez, M. Sanz-Bodi, M. Gutierrez and A. Kraetge, "Knowledge for Interpretation of the Frequency Response Analysis of Power Transformer". ALTAE, November 2009.

[8] J. Velasquez, D. Kolb, "Identification of Transformer-specific Frequency Sub-bands as basis for a Reliable and Automatic Assessment of FRA Result". Conference Proceedings of CMD, 2010.

[9] E. Bjerkan, H. K. Hoidalen, "High frequency FEM based power transformer modeling: Investigation of internal stress due to network-initiated overvoltage", IEEE Transaction on Power Delivery, October 2006.

[10] Mitchell, S.D.; Welsh, J.S., "Modeling Power Transformer to Support the Interpretation of Frequency-Response Analysis", IEEE Transactions on Power Delivery, Vol.26, No.4, October 2011.

[11] Simon A. Ryder, "Methods for comparing frequency response analysis measurements", Conference record of the 2002 IEEE International symposium on electrical insulation, Boston, MA USA, April 2002.

[12] B. Gustavsen, A. Semlyen, "Rational Approximation of Frequency Domain Responses By Vector Fitting ," *IEEE Trans. Power Delivery*, vol. 14, pp. 1052-1061, Dec. 1997.

[13] J. C. Gonzales and E. E. Mombello, "Diagnosis of Power Transformer through Frequency Response Analysis by Poles and Zeros Shifts Identification", IEEE PES T&D, Uruguay, September 2012.

[14] M. Heindl, S. Tenbohlen, "Algorithmic determination of pole-zero representations of power transformer's transfer function for interpretation of FRA data", Proceeding of the 16th International Symposium on High Voltage Engineering, 2009.

IX. BIOGRAPHIES

Jimmy Cesar Gonzales Arispe (S) was born in Cochabamba, Bolivia in April 26, 1984. He received the electrical engineering degree from Universidad Mayor de San Simón, Bolivia, in 2006. He received the Ph.D. degree in electrical engineering from Universidad Nacional de San Juan, Argentina in 2012. He is currently working at Universidad Nacional de San Juan, as a grantee for of post-doctoral position financed by the National Council of Technical and Scientific Research.

Enrique Esteban Mombello (IEEE M'95-SM'00) was born in Buenos Aires, Argentina, in 1957. He received the B.S. degree in electrical engineering and the Ph.D. degree in electrical engineering in 1982 and 1998, respectively from Universidad Nacional de San Juan. He has more than 20 years of experience in research projects including topics like electrical transients and resonance processes within transformers as Researcher of the National Council of Technical and Scientific Research (CONICET, Argentina). He has worked from 1989 to 1991 at the High Voltage Institute of RWTH, Aachen, Germany. He is presently with the Instituto de Energía Eléctrica, National University of San Juan (UE-IEE-UNSJ-CONICET), Argentina, as a Lecturer and Researcher since 1982. His main fields of interest are design, modeling and diagnostics of power transformers, asset management, transformer life management, electromagnetic transients in electric machines and networks, modeling of equipment, corona losses in overhead transmission lines, low frequency electromagnetic fields.